

Fatty Acid Binding Proteins: Potential Chaperones of Cytosolic Drug Transport in the Enterocyte?

Natalie L. Trevaskis · Gary Nguyen · Martin J. Scanlon · Christopher J. H. Porter

Received: 20 December 2010 / Accepted: 5 April 2011 / Published online: 27 April 2011
© Springer Science+Business Media, LLC 2011

ABSTRACT

Purpose Several poorly water-soluble drugs have previously been shown to bind to intestinal (I-FABP) and liver fatty acid binding protein (L-FABP) *in vitro*. The purpose of this study was to examine the potential role of drug binding to FABPs on intestinal permeability and gut wall metabolism *in vivo*.

Methods The intestinal permeability of ibuprofen, progesterone and midazolam (which bind FABPs) and propranolol (which does not) was examined using an autoperfused recirculating permeability model in control rats and rats where FABP levels were upregulated via pre-feeding a fat-rich diet.

Results The intestinal permeability of drugs which bind FABPs *in vitro* was increased in animals where FABP levels were upregulated by prefeeding a high fat diet. The gut wall metabolism of midazolam was also reduced in animals with elevated FABP levels.

Conclusions Consistent with their role in the cellular transport of endogenous lipophilic substrates, FABPs appear to facilitate the intracellular disposition of drug molecules that bind FABPs *in vitro*. Drug binding to FABPs in the enterocyte may also attenuate gut wall metabolism in a manner analogous to the reduction in hepatic extraction mediated by drug binding to plasma proteins in the systemic circulation.

KEY WORDS drug absorption · drug metabolism · fatty acid binding protein · intestinal permeability · poorly water-soluble drugs

ABBREVIATIONS

FABPs fatty acid binding proteins
I-FABP intestinal FABP
iLBP intracellular lipid binding proteins
L-FABP liver FABP

INTRODUCTION

Drug solubility in the gastrointestinal fluids and adequate permeability across the enterocyte are the principle determinants of effective absorption following oral delivery (1,2). Considerable efforts have therefore been directed towards the development of *in vitro* models which allow prediction of *in vivo* dissolution and permeability (3). From the perspective of permeability assessment, attention has focused primarily on the barrier to permeability provided by transport across the apical and/or basolateral membranes of the enterocyte, and the role of membrane transporters as potential conduits (influx transporters) or barriers (efflux transporters) to absorption (4,5). Consideration of partitioning behaviour, however, suggests that for lipophilic drugs, movement out of the lipophilic apical membrane into and across the predominantly aqueous cytoplasm of the enterocyte may also be a significant barrier to cellular transport and therefore absorption.

Endogenous lipophilic molecules (such as dietary-related lipids, bile salts, fat-soluble vitamins and some lipophilic biological messengers) are faced with similar hurdles to cytoplasmic transport. In this case, diffusion is facilitated by interaction with intracellular lipid binding proteins (iLBP),

N. L. Trevaskis · G. Nguyen · C. J. H. Porter (✉)
Drug Delivery, Disposition and Dynamics, Monash Institute
of Pharmaceutical Sciences, Monash University
381 Royal Parade
Parkville, Victoria, Australia 3052
e-mail: Chris.Porter@monash.edu

M. J. Scanlon
Medicinal Chemistry and Drug Action, Monash Institute
of Pharmaceutical Sciences, Monash University
381 Royal Parade
Parkville, Victoria, Australia 3052

including fatty acid binding proteins (FABPs) (6–11), ileal bile acid binding protein (I-BABP) (7), sterol carrier proteins (SCPs) (12) and cellular retinoic acid (CRABP) and retinol binding proteins (RBPs) (6).

Appreciation of the role of iLBPs in the cellular transport of endogenous lipophilic molecules led us recently to explore the potential for iLBPs to act as intracellular chaperones for poorly water-soluble, lipophilic drugs and in particular to explore their potential role in drug absorption. Of the iLBPs, the FABPs were of particular interest, as they are the most abundant proteins in many cells (including enterocytes) and constitute up to 3–6% of cellular protein (13). The nomenclature of FABPs reflects the organ in which they were first identified; however, their distribution, whilst organ specific, is not exclusive. As such, many FABPs are expressed in several tissues, and in the enterocyte both intestinal FABP (I-FABP) and liver FABP (L-FABP) are present in appreciable quantities. I-FABP and L-FABP facilitate the intracellular trafficking of fatty acids (6–8,10,11) and are capable of binding non-fatty acid ligands, including heme, eicosanoids, lyso-phosphatidylcholine and some xenobiotics (6–8). They are also believed to facilitate lipid absorption (7,14–17), to promote lipid trafficking to the endoplasmic reticulum (18), to support passage of lipoproteins from the endoplasmic reticulum to the Golgi apparatus (19), to maintain intracellular sink conditions such that accumulation of toxic concentrations of fatty acid within enterocytes is prevented (7), and to assist lipid transport to the nucleus where interaction with nuclear hormone receptors facilitates transcriptional regulation of lipid metabolism (20,21).

Consistent with their role in the transport of endogenous lipophilic moieties, we have recently shown that I-FABP and L-FABP bind to a range of poorly water-soluble drugs. In particular, drugs with structural similarities to fatty acid, such as the presence of a hydrophobic moiety and a free carboxylic acid group, appear to bind to I-FABP and L-FABP with higher affinity (low micromolar) (22–28). Compounds found to bind FABPs *in vitro* include NSAIDs (fenamates, propionic acid derivatives, indole acids and heteroacyl acetic acid derivatives) and fibrates, both of which commonly exhibit a free carboxylic acid group, and others such as certain steroids and benzodiazepines which do not have a free carboxylic acid group (22,23,26,27). We have subsequently shown that the transmembrane transport of drugs which bind to FABP may be increased by the presence of I-FABP in the acceptor chamber of simple *in vitro* permeability models (PAMPA) (27). These data are consistent with a role for FABPs in the cellular transport of poorly water-soluble drugs, and in drug absorption after oral administration, but to this point *in vivo* evidence of this contention has not been described.

The current study has therefore assessed *in vivo* the role of FABPs in the intestinal absorption and transport of four

model drugs (ibuprofen, progesterone, propranolol and midazolam). An autoperfused rat intestine preparation was used to assess the rate of drug uptake from the jejunum under conditions where FABP expression was modified by pre-feeding a high fat diet. The four model drugs were chosen since they differed in both their affinity for I-FABP and L-FABP and their lipophilicity (Table I). Midazolam was chosen as a model compound which binds FABP *in vitro* and is also subject to Cyp3A4-mediated gut wall metabolism. Midazolam therefore allowed examination of the potential impact of raised levels of FABP on gut wall metabolism. The data suggest that FABPs provide an intracellular binding partner for some drugs and that drug binding to FABP in the cytoplasm of the enterocyte may influence cellular transport and attenuate the extent of gut wall metabolism.

MATERIALS AND METHODS

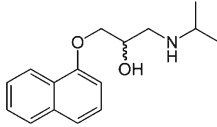
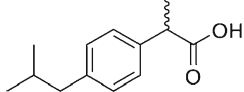
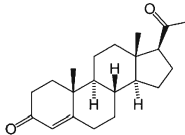
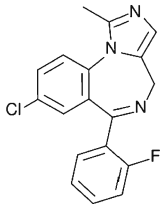
Materials

Midazolam and 4-hydroxy midazolam (Toronto Research Chemicals, Canada), tert-butyl methyl ether (TBME; Merck, Germany), Solvable®, Ultima Gold® and Starscint® scintillation fluid, propranolol L-[4-³H] (24.4 Ci/mmol), polyethylene glycol (PEG) 4000 [¹⁴C] (10–20 mCi/g) (Perkin Elmer Life Sciences, MA, USA), ibuprofen, R (–) [carboxyl-¹⁴C] (50–60 mCi/mmol) and progesterone [1, 2-³H] (52 Ci/mmol) (American Radiolabelled Chemicals, MO, USA), diazepam, propranolol hydrochloride, ibuprofen, progesterone, D-mannitol-1-¹⁴C (40–60 mCi/mmol), mannitol, antipyrine-N-methyl-¹⁴C (1–15 mCi/mmol), antipyrine, sodium hydroxide, acetic acid, sodium acetate, sodium chloride (NaCl), potassium chloride (KCl), calcium chloride (CaCl₂), sodium phosphate dibasic (Na₂HPO₄), sodium phosphate monobasic (NaH₂PO₄·2H₂O) 30% hydrogen peroxide and polyethylene glycol (PEG) 4000 (Sigma Aldrich, Australia) were obtained from listed suppliers. Methanol and acetonitrile (ACN) were analytical reagent grade. Water was obtained from a Millipore milli-Q Gradient A10 water purification system (Millipore, MA, USA).

Choice of Model Drugs

The structure, clog P, clog D_{5.5}, clog D_{7.5} and binding affinity to the single binding site of I-FABP and the first and second binding site of L-FABP for each of the model drugs (propranolol, ibuprofen, progesterone and midazolam) are given in Table I. All drugs are relatively lipophilic in the unionised form with clog P > 3.5. Ibuprofen, however, is ionisable at neutral pH so has a lower clog D_{5.5} and clog D_{7.4}. The binding affinity of each of the drugs for FABP is

Table 1 Physicochemical Properties and I-FABP and L-FABP Binding Affinity (K_i , μM , Mean \pm SD) of Propranolol, Ibuprofen, Progesterone and Midazolam

Compound	Molecular weight	cLogP	cLog $D_{5,5}$	cLog $D_{7,4}$	I-FABP K_i (μM)	L-FABP (site 1) K_i (μM)	L-FABP (site 2) K_i (μM)	Structure
Propranolol	259.34	3.6 ^a	0.7 (65)	1.4 (65)	No binding detected (27)	No binding detected	No binding detected	
Ibuprofen	206.28	3.7 (22)	2.6 (22)	0.77 (27)	58 \pm 8 (27)	47.6 \pm 9.8 (22)	448 \pm 39 (22)	
Progesterone	314.46	4.04 (22)	4.04 (22)	4.04 (27)	20 \pm 4.6 (27)	0.027 \pm 0.0011 (22)	No binding detected (22)	
Midazolam	325.78	3.9 ^a	3.48 ^a	3.92 ^a	12 \pm 3 (midazolam) 20 \pm 7 (4-OH midazolam)	7.9 \pm 0.2 (midazolam) 9.5 \pm 1.1 (4-OH midazolam)	No binding detected	

^a Calculated using ACD/labs v4.56 (Toronto, Canada)

reproduced from previous studies or was determined via displacement of the fluorescent marker, 1-anilinoanthracene-8-sulfonic acid (ANS) from the FABP binding site(s), as described previously (26,27). Propranolol does not bind I-FABP or L-FABP, but has similar lipophilicity to the other probe compounds and was therefore used as a control. Both ibuprofen and midazolam displayed moderate affinity for I-FABP and L-FABP (K_i 5–100 μM). Progesterone has a strong affinity for the first binding site of L-FABP and has a moderate affinity for I-FABP. Ibuprofen, progesterone and midazolam were therefore chosen as model drugs which bind to I-FABP and L-FABP *in vitro*.

Midazolam was also chosen, as it is subject to significant first-pass metabolism in the enterocyte (29,30) and therefore offered the opportunity to probe the impact of FABP binding on intracellular drug metabolism. Ibuprofen (31) is not significantly metabolised during intestinal perfusion. Little has been published describing the gut wall metabolism of propranolol or progesterone. Both, however, are highly metabolised in the liver, and metabolism in the intestine is possible. In the current study, progesterone and propranolol uptake into the intestine and flux into mesenteric blood were explored using radiolabelled materials. In the latter case (i.e., transport into the mesenteric blood), the total flux of radiolabel quantified

likely represents both parent and some proportion of radiolabelled metabolites.

Experimental Outline

Rats were fed either a control diet or a high fat diet to up-regulate the expression of I-FABP and L-FABP in the intestine for 1 week prior to experiments. The protocol employed was similar to those previously utilised to enhance I-FABP and L-FABP expression in the intestine (32,33). The impact of altered expression of I-FABP and L-FABP on the permeability of the model compounds (propranolol, ibuprofen, progesterone and midazolam) across an isolated jejunal segment (including both the rate of uptake into the intestinal segment and rate of transport into the mesenteric blood draining the intestinal segment) and the mass of the drug within the jejunal segment at the conclusion of experiments were subsequently examined. For midazolam, the impact of altered I-FABP and L-FABP expression on the formation of metabolite in the intestine was also assessed.

Animals

All experiments were approved by the local animal ethics committee and were conducted in accordance with the

Australian and New Zealand Council for the Care of Animals in Research and Teaching guidelines. Male Sprague-Dawley rats (280–320 g) were used in all experiments. Rats were fed either a standard diet (AIN93G from Specialty Feeds, Australia, containing 7% fat) or a high fat diet (SF04-019 from Specialty Feeds, Australia, containing 20–23% fat in the form of 2.9% soya oil and 17.1% lard) for 7 days prior to experiments. Rats were fasted overnight prior to experiments to ensure complete absorption and transport of pre-dosed lipids out of enterocytes prior to conduct of permeability experiments. In this way, any acute effects of feeding on drug absorption were avoided.

Surgical Procedures

The rat perfusion model employed involves the *in situ* perfusion of an isolated jejunal segment with recirculating perfusate (via a reservoir) and simultaneous blood collection from the corresponding mesenteric vein branch. The surgical procedures for the *in situ* recirculating rat jejunal perfusion have been described previously (34) and were adapted from the methods of Windmueller and Spaeth (35) and Farraj (36). Briefly, animals were anaesthetised prior to surgery and throughout experiments with a combination of ketamine, xylazine and acepromazine (34). They were maintained on a 37°C heated pad throughout the surgery and subsequent experiment. The right jugular vein of the animal was first cannulated (37). A 10–15 cm segment of jejunum was then cannulated at the proximal and distal ends with sections of Teflon tubing which were subsequently attached to a peristaltic pump (Amersham Biosciences, Inc., Piscataway, NJ). The mesenteric vein draining the intestinal segment was then isolated, the animal heparinized (90 U/kg) via the jugular vein cannula, and the mesenteric vein immediately catheterized. Approximately 0.3 ml/min of blood was continuously drained and collected from the mesenteric vein, and this blood loss was replaced via infusion of 0.3 ml/min fresh heparinized donor blood into the jugular vein via a second peristaltic pump. The donor blood was collected from donor rats immediately before surgery by cardiac puncture. At the end of experiments, rats were killed via intravenous or intraperitoneal injection of 1 ml of 100 mg/ml pentobarbitone.

Intestinal Perfusion Protocol

The peristaltic pump recirculated perfusate from a 37°C jacketed reservoir through the jejunal segment at a rate of 0.6 ml/min. The perfusate buffer consisted of 146.42 mM Na⁺, 4.56 mM K⁺, 1.25 mM Ca²⁺, 0.66 mM HPO₄²⁻, 0.1 mM H₂PO₄, adjusted to pH 6.5 at 37°C. Buffer was perfused through the jejunal segment (and the flow through discarded to waste) for 30 min prior to experiments to enable

the animals to stabilise. After the stabilisation period, air was pumped through the segment in order to remove all fluid inside the intestine. The perfusate buffer was then replaced with a reservoir containing 10 ml of the drug solutions dissolved in perfusate buffer, including 5 µg/ml propranolol (with 0.1 µCi/ml ³H-propranolol), 15 µg/ml ibuprofen (with 0.1 µCi/ml ¹⁴C-ibuprofen), 50 µg/ml progesterone (with 0.1 µCi/ml ³H-progesterone) or 50 µg/ml midazolam. The drug concentrations used were approximately 80% of the maximum solubility of the compounds in the perfusate and, for poorly water-soluble drugs such as these, represent concentrations that might be expected to be attained during *in vivo* dissolution of a range of drug doses. Control experiments were also performed where rats were perfused with 0.6 ml/min of solutions containing 1 mM antipyrine (with 0.1 µCi/ml ¹⁴C-antipyrine), 1 mM mannitol (with 0.1 µCi/ml ¹⁴C-mannitol) or 1 mM PEG4000 (with 0.1 µCi/ml ¹⁴C-PEG4000) in perfusate buffer to assess the integrity of the intestinal preparation to transcellular and paracellular permeability markers and to monitor for changes to water flux into the intestinal segment, respectively. The validity of the model was assessed by comparison of these data to literature values for the same markers (38–42) (see “Results” section).

Animals were perfused with the drug solutions for 1 h. Perfusate samples (50 µl) were taken from the perfusate reservoir at the commencement of the experiment and every 10 min throughout the experiment. Mesenteric blood was collected continuously into tared 1.5 ml Eppendorf tubes which were changed at 5-min intervals. After the blood was collected, the tubes were weighed to calculate the rate of blood flow for each 5-min interval, and plasma was separated from the blood via centrifugation at 3,000 g for 5 min. At the conclusion of the experiment, perfusate buffer was flushed out of the jejunal segment, and the segment was removed, placed in a 20 ml scintillation vial, and frozen at –20°C to enable later measurement of drug concentrations. A small scraping of the intestinal mucosa was also taken from the jejunum approximately 1–2 cm either side of the cannulated segment using a microscope slide, taking care to avoid any tissue damaged via the jejunal cannulation, to enable measurement of the expression of I-FABP and L-FABP. The scrapings were placed in an Eppendorf and immediately snap frozen in liquid nitrogen.

Measurement of Drug Concentrations

Scintillation Counting

Concentrations of ³H-propranolol, ¹⁴C-ibuprofen, ³H-progesterone, ¹⁴C-antipyrine, ¹⁴C-mannitol and ¹⁴C-PEG4000 in the perfusate, plasma, and intestinal segment were measured by scintillation counting. Perfusate (50 µl) and

plasma (100 μ l) samples were prepared for scintillation counting via addition of 2 ml of Starscint® scintillation fluid followed by a 30 s vortex. The entire perfused segments of intestine were prepared for scintillation counting by placing in a 20 ml glass scintillation vial with 2 ml Solvable®, incubating at 40°C for 48 h, adding 200 μ l of 30% H₂O₂, and incubating for 1 h at 50°C. Half of the dissolved tissue solution (1.1 ml) was then transferred into a separate 20-ml glass scintillation vial, 12 ml of Ultima Gold® added to each vial, and the vials vortexed for 30 s. The scintillation counting methods were validated by spiking, in triplicate, blank perfusate, plasma or intestine samples with low, medium or high concentration of each radiolabelled drug. The measured concentrations were within 5% of the nominal concentration.

HPLC of Midazolam and its 4-hydroxy Metabolite

Preparation of Samples. To facilitate quantification of the extent of metabolism of midazolam, an HPLC assay was developed to quantify midazolam and its primary 4-hydroxy metabolite. Perfusate samples were prepared for HPLC analysis via 1/40 (*v/v*) dilution with acetonitrile followed by a 1 min vortex, centrifugation at 3,500 g for 5 min and transfer of 100 μ l of supernatant to a HPLC vial. Plasma samples (300 μ l) were prepared for HPLC analysis in a 10 ml polyethylene (PE) tube via addition of internal standard (750 ng/ml diazepam), followed by a 1 min vortex, addition of 200 μ l 0.1 M NaOH and 4 ml diethylether, a 10 min vortex and centrifugation at 3,000 g for 5 min at room temperature. The samples were then placed in the freezer (-20°C) for 35 min and the supernatant transferred to a new 10 ml PE tube. The supernatant was evaporated to dryness under nitrogen (N-EVAP 112 evaporator, Organomation, MA, USA), reconstituted in 150 μ l of mobile phase (see below) and vortexed for 1 min. One hundred μ l of the resulting samples were transferred to HPLC vials for analysis. Drug concentrations were quantified by comparison to standards obtained by spiking blank plasma with known concentrations of midazolam, 4-hydroxy midazolam and internal standard and processing as above.

A back extraction method was used to prepare samples for HPLC analysis of midazolam and metabolite concentrations in the intestinal sections (~10–15 cm). The intestinal sections were first homogenised in 4 ml ice-cold water (using an IKA-Werke® Eurostar Power Control-Visc 6000 Mixer, Germany). Samples of the homogenate (500 μ l) were then transferred into 10 ml PE tubes containing 5 μ g/ml of internal standard (diazepam). The samples were then vortexed for 1 min, and 1 ml TBME and 20 μ l of 5 M NaOH added. Following a 5-min vortex, the samples were centrifuged at 10,000 g for 10 min at 21°C and frozen for 15 min at -80°C. The resulting TBME layer was transferred to a

clean tube containing 800 μ l of 0.02 M orthophosphoric acid and the samples vortexed for 30 s, centrifuged at 3,200 g for 1 min, and 100 μ l of the aqueous phase carefully removed and placed into HPLC vials containing 7 μ l 1M sodium hydroxide.

HPLC Conditions. The HPLC system consisted of a Waters 2690/5 Alliance module and Waters 486 tuneable absorbance detector (set at a wavelength of 254 nm) controlled via Waters empower software (Waters Corp., Milford, MA). Twenty five μ l samples were injected onto a 150×4.6 mm reverse phase C8 column with a pore size of 5 μ m (Phenomenex Luna®, Phenomenex, Australia) fitted with a Phenomenex security guard RP-C8 precolumn (4×3 mm, Phenomenex, Australia). The mobile phase consisted of 40% (*v/v*) acetonitrile, 5% (*v/v*) methanol and 55% (*v/v*) sodium acetate buffer pH 5.6, and the mobile phase flow rate was 1 ml/min. The total run time was 14 min, and midazolam eluted at 7.7 min, 4-hydroxy midazolam at 4.9 min, and diazepam at 11.0 min.

The HPLC assays for midazolam and 4-hydroxy midazolam were validated by assay of replicate (*n*=4) quality control samples at low, medium and high concentrations on three separate days. The midazolam and 4-hydroxymidazolam assay was accurate (within 10% of target concentration) and precise (co-efficient of variation <10%) for concentrations between 25 and 5,000 ng/ml for diluted perfusate samples and 0.1–10 μ g/ml and 0.5–20 μ g/ml for plasma and intestine samples, respectively. Inter-day variability in precision and accuracy was <10%, and the limit of quantitation was 25 ng/ml for diluted perfusate samples, 100 ng/ml for plasma samples and 0.5 μ g/ml for intestine samples.

Blood:Plasma Ratios

The blood-to-plasma ratios for propranolol, ibuprofen, progesterone, midazolam and 4-hydroxy midazolam were determined by spiking blank blood (1 ml) or plasma (1 ml), in triplicate, with low, medium or high concentrations of the drugs. Plasma was then separated from the blood samples by centrifugation at 3,000 g for 5 min and drug concentrations measured by scintillation counting or HPLC as described above. The blood-to-plasma ratio was calculated from the ratio of the concentration measured in the spiked plasma to the concentration measured in the plasma separated from the spiked blood. The mean blood-to-plasma ratios were subsequently used to convert plasma concentrations from the perfusion experiments into blood concentrations, thus enabling calculation of total drug transport into the mesenteric venous blood.

Measurement of Intestinal mRNA Levels of I-FABP and L-FABP

Whilst the high fat diet protocol utilised here was similar to that previously shown to elevate FABP levels, changes to the levels of expression of I-FABP and L-FABP in the intestine were confirmed in the current study via quantitation of changes in the levels of I-FABP and L-FABP mRNA. Concentrations of I-FABP and L-FABP mRNA in the jejunal mucosal scrapings were measured using a qPCR method described and validated previously (43). RNA was extracted with an RNeasy Mini Kit® (Qiagen Limited, Australia), and cDNA prepared via reverse transcription using an Omniscript® kit with random hexamers (Qiagen Limited, Australia) in accordance with the manufacturer's protocol. The qPCR assays utilised a Taqman assay-on-demand kit for I-FABP (Rn 00565061, fatty acid binding protein 1, FABP 2; Applied Biosystems, NJ) or a Taqman® MGB probe and forward and reverse primers (Applied Biosystems, NJ) for L-FABP with the following sequences: L-FABP probe: 5'-CCCAAAGCTGATATAAT-3', forward primer: 5'-AAGTACCAAGTGCAGAGCC AAGA-3' and reverse primer: 5'-GACAGAAGGGATAGCCCCTCAT-3'. Samples were prepared for qPCR in Taqman® Universal PCR master mix (Applied Biosystems, NJ), and the house-keeping gene was 18S ribosomal RNA (44). Samples were run on a Rotorgene RT-3000 (Corbett Research, Australia) and the data analysed using Rotorgene V5 software. To enhance the accuracy of I-FABP and L-FABP q-PCR measurements, each sample was analysed in triplicate. Additionally, to ensure measurements from different q-PCR runs were cross-comparable, a set of reference samples obtained from the upper, middle and lower small intestine of a fasted rat was analysed in each I-FABP or L-FABP q-PCR run and the expression of I-FABP and L-FABP calculated relative to these reference samples. The reference samples were the same for all animals administered the same drug (i.e., propranolol, ibuprofen, progesterone or midazolam) but not in the animals administered different drugs, such that cross comparison between the groups administered different drugs were not considered accurate and are not reported in this manuscript.

Data Analysis

In pre-study validation experiments, non-specific adsorption of all compounds was observed during 60 min of passage of drug-buffer solutions through the perfusion pump and into the tubing used to perfuse the jejunum. Drug solutions were therefore recirculated through the perfusion tubing at 0.6 ml/min for 60 min prior to commencing perfusion of the jejunum, in order to saturate non-specific adsorption. Drug concentrations in

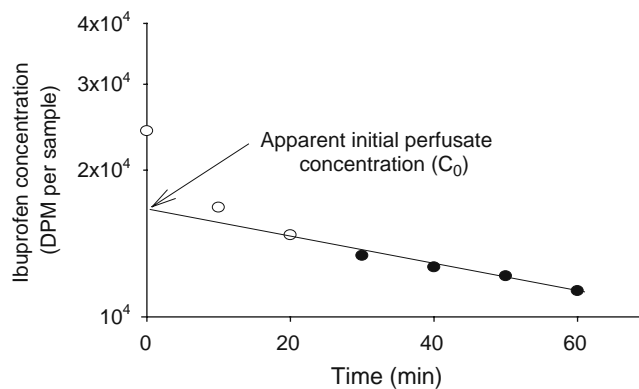


Fig. 1 Typical plot from one animal showing the log concentration of drug (in this case ibuprofen) in the perfusate over time during continuous perfusion of a 10–15 cm segment of rat jejunum with 150 μ g of ¹⁴C-ibuprofen.

the perfusate were then expected to decline log-linearly (i.e., reflecting first-order absorption) throughout the 1 h perfusion of the rat jejunum. For all compounds, however, an initial rapid decrease in perfusate drug concentrations was evident from 0 to 10 min, which was greater than expected and greater than the subsequent log-linear rate of decline in drug concentrations from 20 to 60 min (as depicted in the sample data in Fig. 1). The decline in perfusate concentrations of PEG4000, a non-absorbable marker used to trace changes in water flux, followed a similar pattern with a marked decrease in perfusate concentrations in the first 10 min. The initial decline was therefore not likely to reflect adsorption (since PEG is a hydrophilic material that does not adsorb to plastic tubing). Rather, the decline in drug concentrations during the first 10 min of perfusion was likely the result of dilution/exchange of drug in the perfusate with residual fluid/mucous that remained in the jejunal segment, even after perfusion of air through the jejunal segment. From 20 to 60 min, the concentration of PEG4000 in the perfusate did not change significantly (less than $\pm 2\%$), and as such it was assumed that there was no water flux into or out of the jejunal segment during this period and thus no change in the volume of the perfusate aside from the 50 μ l samples taken by the experimenter every 10 min. Due to the initial dilution effect, perfusate drug concentrations obtained from the 0–10 min period were excluded from the disappearance permeability coefficient calculations.

Recovery of Drug

The mass of drug administered to the animals (D_0) was calculated from the volume of the perfusate (V_M , measured by weight) and the measured drug concentration in the

perfusate (C_M) immediately prior to connecting the jejunum to the perfusion tubing, as per Eq. 1 below:

$$D_0 = V_M \times C_M \quad (1)$$

To correct for the initial rapid dilution and to estimate the true perfusate volume after reconnection of the reservoir after the stabilisation period (i.e., at $t = 0$ min into experiment), the apparent concentration of drug in the perfusate at $t = 0$ min (C_0) was determined by extrapolating a log-linear regression of the measured concentrations in the perfusate from $t = 20$ min to $t = 60$ min to $t = 0$ min (as shown on Fig. 1).

The volume of the perfusate (V_0) at time zero, taking into account dilution, was then calculated from D_0 and C_0 , as per Eq. 2 below:

$$V_0 = D_0 / C_0 \quad (2)$$

The volume of the perfusate at the end of the experiment (V_{60}) was subsequently calculated by subtracting the volume of samples taken (as the PEG400 data suggested that there was no water flux into or out of the intestine during the 20–60 min experimental period). The mass of drug remaining in the perfusate at the end of the 60 min experiment ($D_{60\text{-perfusate}}$) was calculated from the perfusate drug concentration at the end of the experiment (C_{60}) and V_{60} , as per Eq. 3, respectively:

$$D_{60\text{-perfusate}} = C_{60} \times V_{60} \quad (3)$$

The fraction of the mass of drug administered to the animals (D_0) which remained in the perfusate at the end of the experiment was calculated from the ratio of $D_{60\text{-perfusate}}/D_0$.

The fraction of the mass of drug administered to the animals (D_0) which was present in the jejunum segment at the end of the experiment was similarly calculated from the ratio of the mass of drug measured in the intestinal segment ($D_{60\text{-intestine}}$) and D_0 .

The mass of drug (and metabolite for midazolam) transported into blood during each 5 min collection period was calculated from the volume of blood collected (measured by weight) and the concentration of drug (or metabolite) in the blood sample (which was calculated from the measured plasma drug or metabolite concentrations and blood-to-plasma ratios). The cumulative mass of drug (and metabolite) transported into the blood over the 60-min collection period ($D_{60\text{-blood}}$ and $D_{60\text{-metabolite-blood}}$) was calculated from the sum of transport over each 5-min collection period during the 60-min experiment. The fraction of the mass of drug administered to the animals (D_0) which had been transported into the blood by the end of the experiment was similarly calculated from the ratio of $D_{60\text{-blood}}$ and D_0 .

The total recovery of drug was calculated from addition of the mass of drug remaining in the perfusate at the end of the experiment ($D_{60\text{-perfusate}}$), the mass of drug ($D_{60\text{-intestine}}$) and

any metabolite ($D_{60\text{-metabolite-intestine}}$) in the jejunal segment at the end of the experiment, the cumulative mass of drug ($D_{60\text{-blood}}$) and metabolite ($D_{60\text{-metabolite-blood}}$) transported into the blood during the experiment and the mass of drug removed by the experimenter when sampling the perfusate.

Intestinal Extraction Ratio

The extraction ratio (ER) gives an indication of the extent of drug metabolism during passage across the jejunum. The extraction ratio was calculated at the conclusion of experiments as described previously (29,30,34), from the ratio of the sum of the mass of metabolite in the perfusate (which in all cases was zero as no metabolite was detected in perfusate), blood and intestinal tissue to the sum of the mass of both metabolite in the perfusate, blood and intestinal tissue and parent drug in the intestinal tissue and blood, as shown in Eq. 4 below. In all cases, the extraction ratio was normalised to a 10 cm length of jejunum by multiplying by the ratio of 10 and the length of intestine (L) that was perfused.

$$ER = \frac{\sum \text{metabolites}_{\text{perfusate+intestine+blood}}}{\sum \text{metabolites}_{\text{perfusate+intestine+blood}} + \sum \text{parentdrug}_{\text{intestine+blood}}} \times \frac{10}{L} \quad (4)$$

The fraction of the mass of drug in the intestinal perfusate, jejunal segment or mesenteric blood which was present as metabolite was calculated from the ratio of metabolite to parent plus metabolite in the perfusate, jejunal segment and blood.

Permeability Co-efficients

Permeability co-efficients were calculated as described previously for recirculating perfusion models (34). The uptake rate constant (K_u , s^{-1}) for the drugs was calculated from the negative slope of a plot of \log_e of the mass of drug remaining in the intestinal perfusate (D_i) over the 20–60 min time period. The apparent permeability co-efficients of the drugs based on disappearance from the intestinal perfusate (disappearance P_{app} , cm/s) were calculated using K_u (s^{-1}), V_0 (cm^3) and the surface area of the perfused jejunal segment (A , cm^2) (Eq. 5). The surface area (A) was calculated by multiplying the diameter by the length of the perfused intestinal segment as described previously (34).

$$\text{Disappearance } P_{app} = \frac{V}{A} \cdot K_u \quad (5)$$

The apparent permeability co-efficients of the drugs based on appearance in venous blood (appearance P_{app} , cm/sec) were calculated using A (cm^2), C_0 (nmol/ml) and

the rate of drug appearance in venous blood (dX/dt , nmol/s), as per Eq. 6:

$$\text{Appearance } P_{\text{app}} = \frac{dX/dt}{A \cdot C_0} \quad (6)$$

Statistical Analysis

Comparisons between apparent permeability co-efficients, extraction ratios, fractional metabolism and drug recovery in blood, intestinal tissue or perfusate of rats fed the control or high fat fed diet were made by student's *t*-test where $P < 0.05$ was considered significant. The SPSS for Windows V11.5.0 software package (SPSS Inc, Chicago, IL) was used for all statistical analyses.

RESULTS

Model Integrity

The integrity of the model was confirmed by mean mesenteric blood flow rates of 0.27–0.43 ml/min and the presence of negligible water flux after 10 min as the perfusate concentrations of PEG4000 (a non absorbable marker) changed by less than 2% during the 20–60-min sampling time in five replicate validation experiments. The permeability of mannitol and antipyrine, which are standard markers of passive paracellular and transcellular permeability, were also within the literature range. The mean appearance P_{app} for mannitol ($n=3$) was $1.03 \pm 0.14 \times 10^{-6}$ cm/sec. This compares with literature values of $1-3.4 \times 10^{-6}$ cm/sec (41,42). The disappearance P_{app} could not be accurately measured, as disappearance was extremely low for this low permeability marker. The mean disappearance P_{app} and appearance P_{app} for antipyrine ($n=4$) were $44 \pm 9 \times 10^{-6}$ and $31 \pm 1 \times 10^{-6}$ cm/sec, which compare to literature values for disappearance P_{app} ranging from 47 to 73×10^{-6} cm/sec (38–42). Literature values for the appearance P_{app} for antipyrine could not be located.

The validity of perfusion experiments was further confirmed by recovery (mass balance) of 97–103% of the dose of ibuprofen and propranolol and 83–116% of the dose of progesterone in the perfusate, blood and intestine samples of control animals and animals where FABP levels were elevated by prefeeding a high fat diet. As expected, the recovery of midazolam was lower (59–69% of the dose), since not all midazolam metabolites were quantified.

Jejunal Expression of I-FABP and L-FABP

Table II compares the levels of I-FABP and L-FABP mRNA in jejunal samples from control or high fat fed rats,

Table II Relative Increase in I-FABP and L-FABP mRNA (Fold Increase) in Jejunal Samples Taken from High Fat Fed Rats when Compared to Control Rats. Samples Were Taken Immediately Following Continuous Perfusion of Jejunal Segments for 60 min with Either 150 μg of ^{14}C -ibuprofen, 50 μg of ^3H -progesterone, 500 μg of ^3H -propranolol or 500 μg of Midazolam Dissolved in 10 ml Buffer. Data Represent Mean \pm SEM for $N=4$ or 5 Rats

Drug	I-FABP	L-FABP
Ibuprofen	3.2 ± 1.7	1.8 ± 0.4^a
Progesterone	1.7 ± 0.7	1.7 ± 0.2^a
Propranolol	1.5 ± 0.4^a	1.9 ± 0.5^a
Midazolam	1.7 ± 0.4^a	1.9 ± 0.8^a

^a Statistically greater in the group fed the high fat diet ($p < 0.05$)

taken immediately after completing the jejunal perfusions with ibuprofen, progesterone, propranolol or midazolam. I-FABP and L-FABP mRNA levels were ~ 1.5 –2-fold greater in the high fat fed rats perfused with each of the drugs, although significant ($\alpha < 0.05$) increases in I-FABP mRNA were only seen in the high fat fed rats perfused with propranolol and midazolam due to the variability in measurements in the rats administered ibuprofen and progesterone. L-FABP mRNA increased significantly ($\alpha < 0.05$) in the high fat fed rats perfused with all of the different drugs. These results confirm that the I-FABP and L-FABP mRNA levels were increased by pre-feeding the high fat diet for 7 days, consistent with previous reports which have shown parallel increases in both mRNA and I-FABP and L-FABP after lipid pre-feeding (20,33).

Drug Disappearance from the Intestinal Lumen

Drug absorption from the intestinal lumen was assessed from the disappearance P_{app} (Table III) and plots of the mass of drug remaining in the perfusate over time (Fig. 2). The disappearance of ibuprofen, progesterone and midazolam from the perfusate was significantly greater in the animals where FABP levels were increased by lipid pre-feeding when compared to the control rats as assessed by a significantly greater disappearance P_{app} (Table III) and a more rapid drop in perfusate drug concentrations over time during the intestinal perfusion (Fig. 2). In contrast, the disappearance P_{app} for propranolol was not statistically different in the two groups (Table III). The disappearance P_{app} for all test compounds was similar to or higher than that of the control transcellular marker antipyrine ($44 \pm 9 \times 10^{-6}$ cm/sec) suggesting that all had relatively high intestinal permeability.

Drug Accumulation in the Intestine

The proportion of the drug dose which was recovered in the perfused intestinal segment at the end of the experiment

Table III Disappearance P_{app} ($\times 10^6$ cm/sec) of Drug from the Intestinal Perfusate, Appearance P_{app} ($\times 10^6$ cm/sec) of Drug in the Mesenteric Blood and % of the Mass of Drug Perfused Through the Intestinal Segment Remaining in the Intestinal Segment (% of dose/g of Intestine) After 60 min of Continuous Perfusion of 10–15 cm Segments of Rat Intestine with Either 150 μ g of 14 C-ibuprofen, 50 μ g of 3 H-progesterone, 500 μ g of 3 H-propranolol or 500 μ g of Midazolam Dissolved in 10 ml Buffer. Rats were Fed Either Control or High Fat Diets for 7 Days Prior to the Studies and Mesenteric Blood was Collected Via a Cannula Placed in a Blood Vessel Draining Only the Perfused Intestinal Segment. Data Represent Mean \pm SEM for $N=4-6$ Rats

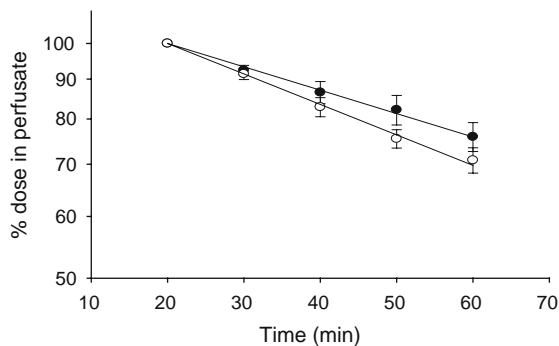
Drug	Group	Disappearance P_{app}	Appearance P_{app}	% of dose per g of intestinal segment
Ibuprofen	Control diet	97 \pm 19	70 \pm 12	2.3 \pm 0.2
	High fat diet	158 \pm 10 ^a	116 \pm 23 ^a	3.1 \pm 0.6 ^a
Progesterone	Control diet	55 \pm 18	49 \pm 3	12.3 \pm 1.4
	High fat diet	129 \pm 22 ^a	22 \pm 3 ^a	9.3 \pm 4.0
Propranolol	Control diet	42 \pm 9	10.9 \pm 2.2	11.1 \pm 1.6
	High fat diet	30 \pm 5	7.7 \pm 0.6	9.3 \pm 0.2
Midazolam	Control diet	143 \pm 32	37 \pm 5	3.3 \pm 0.2
	High fat diet	239 \pm 41 ^a	41 \pm 7	4.8 \pm 0.5 ^a

^aSignificantly different from control diet ($\alpha < 0.05$)

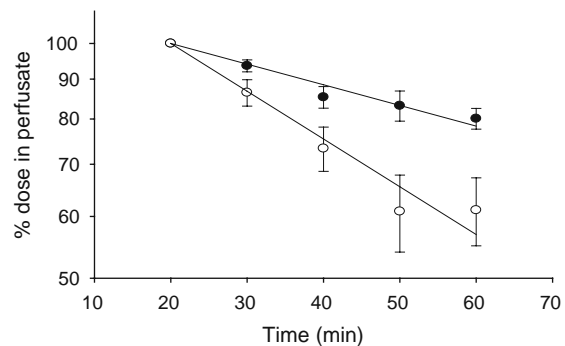
(i.e., after 60 min of perfusion) is given in Table III. Data have been normalised per gram of tissue to allow comparison across groups where the length of the perfused segment varied slightly. For both ibuprofen and midazolam,

significantly more drug accumulation was evident in the intestinal segments of animals where FABP levels were increased by the high fat diet, consistent with the greater uptake (disappearance P_{app}) of these drugs from the

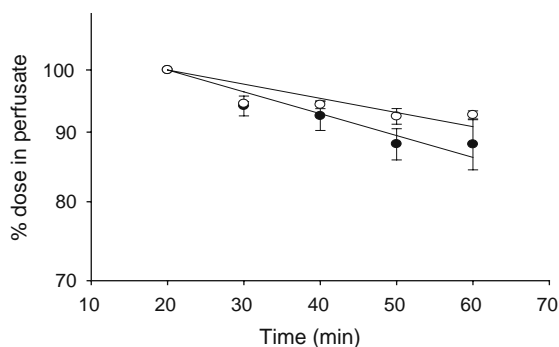
a) Ibuprofen



b) Progesterone



c) Propranolol



d) Midazolam

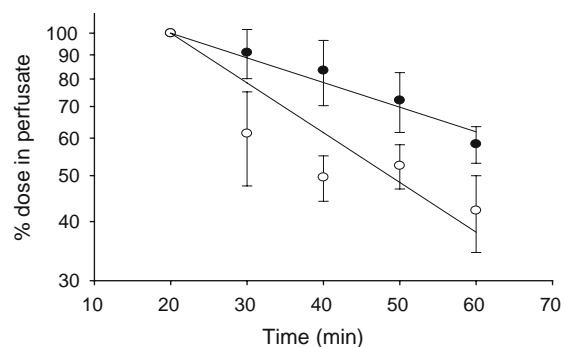


Fig. 2 % of the drug dose remaining in the intestinal perfusate (represented on log scale) over time (min) during continuous perfusion of a 10–15 cm segments of rat intestine with either **a** 150 μ g of 14 C-ibuprofen, **b** 50 μ g of 3 H-progesterone, **c** 500 μ g of 3 H-propranolol or **d** 500 μ g of midazolam dissolved in 10 ml buffer. Rats were fed either a control diet (\bullet) or a high fat diet (\circ) for 7 days prior to the studies. The data are normalised to 100% at $t=20$ min. Data represent mean \pm SEM for $n=4-6$ rats. Note that mean regression lines are provided here as a visual guide, however disappearance P_{app} were calculated by performing a regression of data from individual rats with subsequent averaging of the individual data.

intestinal perfusate (Table III). In contrast, drug accumulation in the intestinal segment in the progesterone and propranolol groups was not significantly different in the high fat fed rats when compared to control.

Drug Appearance in the Mesenteric Blood

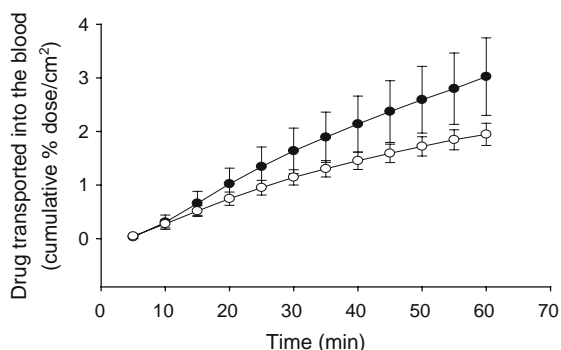
Drug appearance in the mesenteric blood is a function of both the rate of drug uptake from the intestinal perfusate and transport of drug across the enterocyte. Drug appearance was assessed from the appearance P_{app} (Table III) and the plots showing the cumulative transport of drug into the mesenteric blood (normalised per unit surface area of intestine perfused) over time (Fig. 3). For ibuprofen, the appearance P_{app} was significantly greater ($\alpha < 0.05$) in animals where FABP levels were increased by pre-feeding the high fat diet when compared to control rats. The increase in transport of ibuprofen into the mesenteric blood in the high fat fed rats was consistent with increased disappearance P_{app} from the intestinal perfusate and greater accumulation of ibuprofen in the intestinal tissue when compared to control rats (Table III). In contrast, the appearance P_{app} for progesterone into the blood (Table III) was significantly lower ($\alpha < 0.05$) in

high fat fed rats when compared to control rats, in spite of the increase in absorption from the perfusate (Fig. 2). For propranolol and midazolam, the appearance P_{app} (Table III) was not statistically different in the high fat fed and control groups (Table III and Fig. 3).

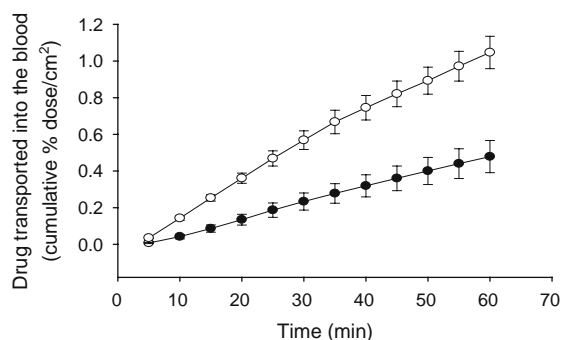
Midazolam Metabolism

Table IV provides a summary of the mass of midazolam and its 4-hydroxy metabolite that was absorbed from the perfusate, transported into the mesenteric blood and recovered in the intestinal segment at the end of the experiment. In this case the intestinal recovery data are provided as the percent dose recovered in each perfused intestinal segment (rather than the data normalised per gram presented in Table III), since this allowed appreciation of mass balance across the experiment. For the midazolam dosed groups, however, the length of the perfused segment did not vary significantly across the high fat fed group and control, allowing direct comparison of intestinal uptake data. Consistent with the disappearance P_{app} data in Table III, the percent dose absorbed from the perfusate was significantly higher in the animals where FABP

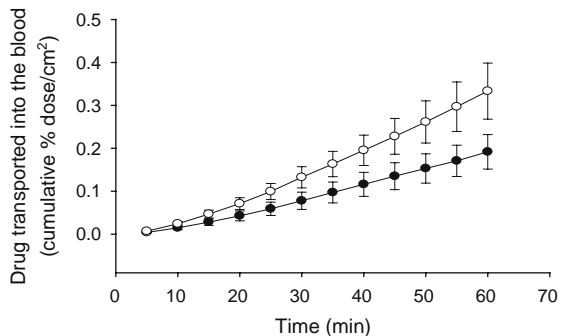
a) Ibuprofen



b) Progesterone



c) Propranolol



d) Midazolam

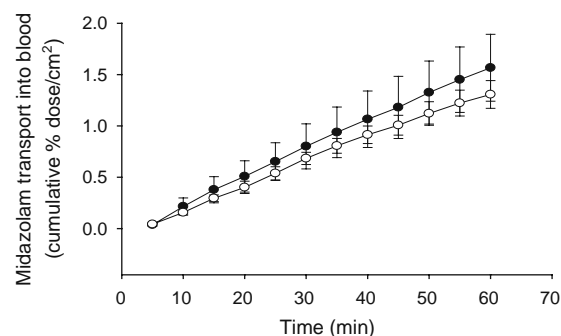


Fig. 3 % of the drug mass contained within the intestinal perfusate at $t = 0$ min (ie dose) which is transported into the mesenteric blood per unit surface area of intestine perfused (% of dose/cm²) over time (min) during continuous perfusion of 10–15 cm segments of rat intestine with either **a** 150 μg of ¹⁴C-ibuprofen, **b** 50 μg of ³H-progesterone, **c** 500 μg of ³H-propranolol or **d** 500 μg of midazolam dissolved in 10 ml buffer. Rats were fed either a control diet (○) or a high fat diet (●) for 7 days prior to the studies. Data represent mean \pm SEM for $n = 4$ –6 rats.

Table IV % of the Mass of Midazolam Contained Within the Intestinal Perfusate at $t=0$ min (ie Dose) Which was Absorbed from the Intestinal Perfusate, Transported into the Mesenteric Blood or Recovered in the Perfused Intestinal Segment as Parent Midazolam or the 4-hydroxy (OH) Midazolam Metabolite After 60 min of Continuous Perfusion of 10–15 cm Segments of Rat Jejunum with 500 μg of Midazolam Dissolved in 10 ml Buffer. Rats were Fed Either a Control or High Fat Diet for 7 days Prior to the Studies and Mesenteric Blood was Collected Via a Cannula Placed in a Blood Vessel Draining Only the Perfused Intestinal Segment. Data Represent Mean \pm SEM for $N=4$ or 5 Rats

	% Absorbed from Perfusate ^b		% Recovered in Intestine			% Transported into Mesenteric Blood		
	Midazolam	Total	Midazolam	4OH-midazolam	Total	Midazolam	4OH-midazolam	Total
Control diet	52.3 \pm 4.9	52.3 \pm 4.9	3.6 \pm 0.3	1.8 \pm 0.2	5.4 \pm 0.4	17.1 \pm 1.0	1.9 \pm 0.6	19.0 \pm 1.4
High fat diet	67.4 \pm 8.2 ^a	67.4 \pm 8.2 ^a	5.4 \pm 0.6	2.2 \pm 0.3	7.6 \pm 0.6	21.1 \pm 4.0	0.6 \pm 0.2 ^a	21.7 \pm 4.1

^aSignificantly different from control diet ($\alpha < 0.05$)

^b $< 0.1\%$ dose equivalent of 4OH-midazolam was recovered in the perfusate throughout the experiment

levels were raised by the high fat diet. In contrast, no significant differences were evident in intestinal accumulation or transport into mesenteric blood, although in both cases slightly higher values were evident in the high fat fed groups.

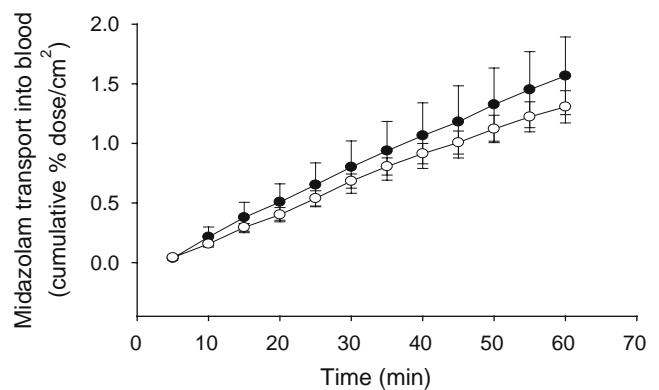
The 4-hydroxy metabolite of midazolam was not detectable in the perfusate throughout the experiment. However, metabolite was evident in both intestinal segments (Table IV) and the mesenteric blood (Fig. 4). In animals where FABP levels were elevated by the high fat diet, significantly less metabolite was recovered in mesenteric blood; however, no significant differences in metabolite recovery were evident in the intestine when compared with control animals. Correcting the extent of metabolism for total drug plus metabolite transport into mesenteric blood revealed a significant difference in the proportion of the total mass contributed by the 4-hydroxy metabolite in the animals with elevated FABP levels (3.1%) when compared to control (11.0%). The midazolam extraction ratio was also significantly reduced in high fat fed animals (Table V).

DISCUSSION

Interest in the mechanisms of drug permeability across the enterocyte has largely focussed on membrane transport for small molecules (45,46) and intracellular trafficking pathways for macromolecular and particulate constructs. In contrast, relatively little has been published on the mechanisms by which small molecule drugs pass across the cytoplasm of the enterocyte during intestinal absorption. Physicochemical drivers, however, suggest that partition into, and diffusion across, the primarily aqueous cytoplasm represents a potential barrier to the cellular transport of poorly water-soluble drugs. In the case of dietary lipids and lipophilic nutrients (47), cytosolic transport is facilitated by intracellular lipid binding proteins such as I-FABP and L-FABP (7,9), and in light of this, we have previously shown that some poorly water-soluble drugs (and in particular those with structural similarities to fatty acids

such as the presence of hydrophobic and carboxylic acid moieties) can bind to both I-FABP (26–28) and L-FABP (22,23) *in vitro*. The current study further suggests that drug

a) Midazolam



b) 4-OH Midazolam

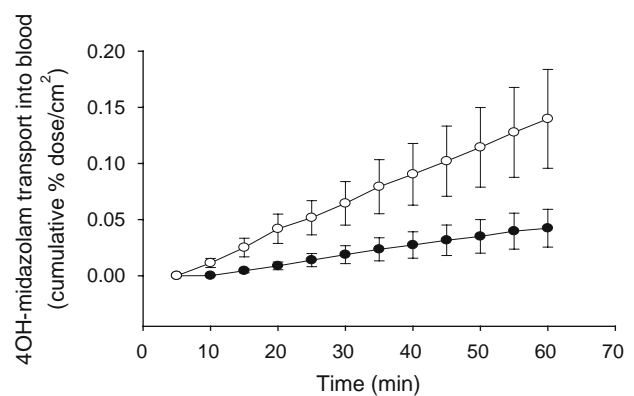


Fig. 4 % of the mass of midazolam contained within the intestinal perfusate at $t=0$ min (ie dose) which is transported into the mesenteric blood per unit surface area of intestine perfused ($\% \text{ dose}/\text{cm}^2$) over time (min) as either **a** parent midazolam or **b** the 4-hydroxy midazolam metabolite during continuous perfusion of 10–15 cm segments of rat intestine with 500 μg of midazolam dissolved in 10 ml buffer. Rats were fed either a control diet (o) or a high fat diet (●) for 7 days prior to the studies. Data represent mean \pm SEM for $n=4$ or 5 rats.

binding to FABPs may influence drug transport across the enterocyte and has the potential to alter access to intracellular sites of drug metabolism.

Fasted levels of expression of I-FABP and L-FABP are generally higher in the duodenum and jejunum (where the majority of lipid absorption occurs) when compared to the ileum (32,43,48), and as such the focus in the current studies was on drug absorption and transport in the jejunum. Animals with varying levels of intestinal FABP were generated by pre-feeding either a high fat diet (20–23% *w/w* fat) or a control diet (7% fat) for 7 days. An increase (1.5–2-fold, Table II) in I-FABP and L-FABP expression was evident in the lipid-fed group, consistent with previous studies that have similarly shown that feeding a high fat diet (ranging between 20% and 40% fat by weight or total calories) to mice or rats for anywhere from 3 to 31 days leads to an approximate 1.3–1.5-fold increase in I-FABP and/or L-FABP expression in the jejunum and ileum (20,32,33,48–50). In previous studies, we have also found that the expression of I-FABP and L-FABP in the duodenum, jejunum and ileum may be up-regulated within as little as 2–5 h in rats administered 20 mg/h of oleic acid intraduodenally (43). The use of lipid pre-feeding as a mechanism of up-regulation of intestinal I-FABP and L-FABP (presumably via fatty acid stimulation of PPAR α (48,51,52,53)) is therefore well documented, and the increases in FABP mRNA documented here are consistent with increases in levels of both mRNA and protein documented previously.

Elevating enterocyte FABP levels by feeding the high fat diet increased intestinal uptake from the luminal perfusate for ibuprofen, progesterone and midazolam (which bind to FABP) but not propranolol (which does not bind to FABP) (Table III, Fig. 2). This is consistent with a role for FABP in drug absorption and is also consistent with a recent study from this laboratory which examined the transport of drugs with differing lipophilicities (including ibuprofen, progesterone and propranolol) in an *in vitro* membrane permeability model (PAMPA), where the donor chamber (representing the intestinal lumen) contained buffer, and the acceptor chamber (representing the cell cytoplasm) contained buffer with or without I-FABP (27). In these studies, increased transport of drugs which bind FABP (such as ibuprofen and progesterone) from the donor to the acceptor chamber was evident in the presence of I-FABP in the receptor chamber, but no change was observed in the transport of propranolol. Transport was particularly enhanced for highly lipophilic drugs with high affinity for FABP (for example the transport of progesterone was enhanced more so than ibuprofen), reflecting an increased affinity for lipophilic molecules for the absorptive membrane when compared with the aqueous environment of the acceptor chamber (and therefore an increased need for a binding partner to assist solubilisation).

In the current studies, increasing FABP levels by prefeeding a high fat diet also enhanced ibuprofen but not propranolol appearance in mesenteric blood, consistent with the disappearance of these compounds from the perfusate (Table III). However, the same was not true for progesterone, where appearance in the mesenteric blood was significantly reduced in the high fat-fed animals when compared to controls, and for midazolam, where transport into the mesenteric blood was not significantly different in either group.

In the case of progesterone, the increased uptake into intestinal segments with raised FABP levels coupled to a decrease in transport out of the intestine into the mesenteric blood was surprising. A possible explanation was the potential for high affinity binding to FABP within the enterocyte to lead to intracellular progesterone accumulation, in turn reducing transport into the blood. However, measurement of the quantity of radioactivity present in the perfused intestinal segment at the end of the experiment did not show an increase in progesterone levels in the high fat, fed group. Overall recovery in the progesterone high fat-fed group was slightly low ($83 \pm 9\%$); therefore, the lack of increase in progesterone in the gut wall (which was expected based on the difference in disappearance and appearance P_{app} data) may have reflected errors in mass balance. Recovery in the other experimental groups, however, was good and pre-study assay validation indicated that the tissue assay was robust. The lower recovery in the progesterone group was therefore drug specific. Little has been published detailing the metabolism of progesterone in the enterocyte, although it is likely to be significant, as the bioavailability of progesterone is low and has been attributed to both poor absorption and extensive first-pass metabolism (54). Under these circumstances, extensive metabolism of the radiolabelled construct in the gut wall may have led to liberation of the tritium label. Leaching of radiolabel via the intestinal submucosa to other segments of the intestine (which were not quantified) may therefore explain the lack of gut wall accumulation. Due to the complexity of progesterone metabolic pathways, further efforts to explore the impact of gut wall metabolism on disposition were not attempted.

In contrast, the metabolic profile of midazolam is well defined and is characterised in large part by hydroxylation by Cyp3A4 in both the intestine and liver (29,55). The major products of gut wall metabolism of midazolam are 4-hydroxy midazolam and 1-hydroxy midazolam, and there is conflicting evidence to suggest whether 4-hydroxy or 1-hydroxy midazolam is the major intestinal metabolite (29,30,56,57). In the current study, levels of the 4-hydroxy-metabolite were used to indicate the extent of metabolism.

The formation of the 4-hydroxy metabolite was significantly lower in the high fat-fed group when assessed by the ratio of metabolite to parent present in the jejunum and mesenteric blood and the overall extraction ratio (Table V). It seems likely, therefore, that midazolam binding to FABP in the enterocyte promoted uptake into the cell but reduced drug access to intracellular metabolic enzymes via a reduction in the intracellular free concentration.

The differences in 4-hydroxy midazolam levels were most evident in mesenteric blood, rather than the intestinal tissues. The *in vitro* binding data suggest similar FABP binding affinities for midazolam and the 4-hydroxy metabolite (Table I). It is possible, therefore, that metabolite that is liberated in the enterocyte subsequently binds to FABP, reducing appearance in mesenteric blood. Enhanced binding of the metabolite to elevated levels of FABP in the high fat-fed group, however, cannot entirely explain the reduced levels of metabolite in the mesenteric blood, since the total mass of metabolite formed (in mesenteric blood plus intestinal tissue) was lower in the high fat-fed group. Increases in FABP levels in the enterocyte therefore appear to reduce metabolism and to limit partition of the metabolite out of the enterocyte into mesenteric blood.

High fat diets are known to influence the intestinal expression of many proteins which influence lipid absorption (e.g. CD36/FAT (32,58), FATP4 (50), Npc111 (59), Abca1 (59), Abcg5 (59), Abcg8 (59), MGAT2 (60), FAS (61), ACC (61), MTP (50,61), ApoAIV(50,61), ApoB (61,62), ApoCIII (61) and CRBPII (63)) as a result of coordinate regulation of these proteins by nuclear hormone receptors (64). The high fat diet administered to the animals in the current study may therefore have led to changes in intestinal permeability that are unrelated to FABP binding. Alternatively, changes to lipid transporter expression may have altered intracellular drug trafficking

by changing the patterns of intracellular disposition of lipids with which lipophilic drugs may associate. However, significant intracellular lipid accumulation is unlikely in the current studies given the evidence that lipid does not accumulate in high fat-fed animals (50) and that all the animals utilised here were fasted overnight prior to the conduct of the permeability studies. The observed changes in intracellular transport were also only evident for drugs which bind I-FABP and/or L-FABP, and the transport of a similarly lipophilic model compound that does not bind FABP (propranolol) was unaltered.

In the case of the observed protection from gut wall metabolism of midazolam in the high fat-fed rats, it is also possible that the administered lipids may have directly inhibited the activity of Cyp3A4. Hirunpanich *et al.* demonstrated that 10–200 μM docosahexanoic acid inhibited the metabolism of midazolam in perfused everted gut sections and that 100 mg/kg docosahexanoic acid inhibited the metabolism of midazolam following oral administration to rats (66). However, in the same study more typical dietary lipids such as 100 mg/kg olive oil had no effect on Cyp activity. Cyp inhibition is therefore likely to be highly lipid specific and to require co-location of lipid and drug in the enterocyte during absorption. In contrast, in the current studies, animals were fasted overnight prior to the conduct of permeability studies.

In summary, the current study has shown that pre-feeding rats with a lipid-rich diet leads to upregulation of I- and L-FABP mRNA in rats and that this occurs in parallel with changes to intestinal permeability of ibuprofen, progesterone and midazolam (drugs which bind to FABPs) but not propranolol (which does not bind FABPs). The data suggest that consistent with their role in the cellular transport of endogenous lipophilic substrates, FABPs facilitate the absorption and intracellular disposition of drug molecules that bind FABPs *in vitro*. The extent of gut wall metabolism of midazolam is also reduced in animals with elevated FABP levels, suggesting that drug binding to FABPs in the enterocyte may attenuate gut wall metabolism in a manner analogous to the reduction in hepatic extraction mediated by drug binding to plasma proteins in the systemic circulation. Finally, it should be noted that the intent of the current studies was to explore the potential role of FABPs in intracellular drug solubilisation and transport. In doing so, we employed a model of lipid pre-feeding to manipulate cellular FABP levels. Whilst the increases in FABP levels generated here by lipid feeding are therefore appropriate for use as a tool to explore the role of FABPs in cellular transport, the absolute differences in FABP expression and changes to drug permeability were moderate. It remains to be seen, therefore, whether the differences in absorption observed under differing feeding conditions have clinical significance.

Table V Fraction (as a %) of the Mass of Midazolam Contained Within the Intestinal Perfusate or Perfused Intestinal Segment or Transported into the Mesenteric Blood that was Present as the 4-hydroxy Metabolite and the Extraction Ratio for Midazolam Transport Across Intestinal Segments after 60 min of Continuous Perfusion of 10–15 cm Segments of Rat Jejunum with 500 μg of Midazolam Dissolved in 10 ml Buffer. Rats were Fed Either a Control or High Fat Diet for 7 Days Prior to the Studies and Mesenteric Blood was Collected Via a Cannula Placed in a Blood Vessel Draining only the Perfused Intestinal Segment. Data Represent Mean \pm SEM for $N=4$ or 5 Rats

	Fraction present as metabolite (%)			Extraction ratio
	Perfusate	Intestine	Blood	
Control diet	<0.2	32.8 \pm 1.9	11.0 \pm 3.3	11.2 \pm 0.9
High fat diet	<0.2	29.1 \pm 3.6	3.1 \pm 0.8 ^a	7.1 \pm 1.1 ^a

^a Significantly different from control diet ($\alpha < 0.05$)

ACKNOWLEDGMENTS

We would like to thank Dr. Sara Chuang and Dr. Tony Velkov for performing the experiments to measure the FABP binding affinity of the model drugs.

REFERENCES

- Wu CY, Benet LZ. Predicting drug disposition via application of BCS: transport/absorption/ elimination interplay and development of a biopharmaceutics drug disposition classification system. *Pharm Res.* 2005;22(1):11–23.
- Amidon GL, Lennernas H, Shah VP, Crison JR. A theoretical basis for a biopharmaceutics drug classification: the correlation of *in vitro* drug product dissolution and *in vivo* bioavailability. *Pharm Res.* 1995;12(3):413–20.
- Burton PS, Goodwin JT. Solubility and permeability measurement and applications in drug discovery. *Comb Chem High Throughput Screen.* 2010;13(2):101–11.
- Ito K, Suzuki H, Horie T, Sugiyama Y. Apical/basolateral surface expression of drug transporters and its role in vectorial drug transport. *Pharm Res.* 2005;22(10):1559–77.
- Benet LZ, Cummins CL. The drug efflux-metabolism alliance: biochemical aspects. *Adv Drug Deliv Rev.* 2001;50 Suppl 1:S3–S11.
- Besnard P, Niot I, Poirier H, Clement L, Bernard A. New insights into the fatty acid-binding protein (FABP) family in the small intestine. *Mol Cell Biochem.* 2002;239(1–2):139–47.
- Agellon LB, Toth MJ, Thomson AB. Intracellular lipid binding proteins of the small intestine. *Mol Cell Biochem.* 2002;239(1–2):79–82.
- Storch J, McDermott L. Structural and functional analysis of fatty acid-binding proteins. *J Lipid Res.* 2009;50(Suppl):S126–31.
- Kaczocha M, Glaser ST, Deutsch DG. Identification of intracellular carriers for the endocannabinoid anandamide. *Proc Natl Acad Sci USA.* 2009;106(15):6375–80.
- Luxon BA. Inhibition of binding to fatty acid binding protein reduces the intracellular transport of fatty acids. *Am J Physiol.* 1996;271(1 Pt 1):G113–20.
- Hung DY, Burczynski FJ, Chang P, Lewis A, Masci PP, Siebert GA, *et al.* Fatty acid binding protein is a major determinant of hepatic pharmacokinetics of palmitate and its metabolites. *Am J Physiol Gastrointest Liver Physiol.* 2003;284(3):G423–33.
- Murphy EJ. Sterol carrier protein-2: not just for cholesterol any more. *Mol Cell Biochem.* 2002;239(1–2):87–93.
- Paulussen RJ, van Moerkerk HT, Veerkamp JH. Immunochemical quantitation of fatty acid-binding proteins. Tissue distribution of liver and heart FABP types in human and porcine tissues. *Int J Biochem.* 1990;22(4):393–8.
- Vassileva G, Huwyler L, Poirier K, Agellon LB, Toth MJ. The intestinal fatty acid binding protein is not essential for dietary fat absorption in mice. *FASEB J.* 2000;14(13):2040–6.
- Newberry EP, Kennedy SM, Xie Y, Luo J, Davidson NO. Diet-induced alterations in intestinal and extrahepatic lipid metabolism in liver fatty acid binding protein knockout mice. *Mol Cell Biochem.* 2009;326(1–2):79–86.
- Woudstra TD, Drozdowski LA, Wild GE, Clandinin MT, Agellon LB, Thomson AB. The age-related decline in intestinal lipid uptake is associated with a reduced abundance of fatty acid-binding protein. *Lipids.* 2004;39(7):603–10.
- Agellon LB, Li L, Luong L, Uwiera RR. Adaptations to the loss of intestinal fatty acid binding protein in mice. *Mol Cell Biochem.* 2006;284(1–2):159–66.
- Karsenty J, Helal O, de la Porte PL, Beauclair-Deprez P, Martin-Elyazidi C, Planells R, *et al.* I-FABP expression alters the intracellular distribution of the BODIPY C16 fatty acid analog. *Mol Cell Biochem.* 2009;326(1–2):97–104.
- Neeli I, Siddiqi SA, Siddiqi S, Mahan J, Lagakos WS, Binas B, *et al.* Liver fatty acid-binding protein initiates budding of pre-chylomicron transport vesicles from intestinal endoplasmic reticulum. *J Biol Chem.* 2007;282(25):17974–84.
- Poirier H, Niot I, Monnot MC, Braissant O, Meunier-Durmort C, Costet P, *et al.* Differential involvement of peroxisome-proliferator-activated receptors alpha and delta in fibrate and fatty-acid-mediated inductions of the gene encoding liver fatty-acid-binding protein in the liver and the small intestine. *Biochem J.* 2001;355(Pt 2):481–8.
- Schroeder F, Petrescu AD, Huang H, Atshaves BP, McIntosh AL, Martin GG, *et al.* Role of fatty acid binding proteins and long chain fatty acids in modulating nuclear receptors and gene transcription. *Lipids.* 2008;43(1):1–17.
- Chuang S, Velkov T, Horne J, Porter CJ, Scanlon MJ. Characterization of the drug binding specificity of rat liver fatty acid binding protein. *J Med Chem.* 2008;51(13):3755–64.
- Chuang S, Velkov T, Horne J, Wielens J, Chalmers DK, Porter CJ, *et al.* Probing the fibrate binding specificity of rat liver fatty acid binding protein. *J Med Chem.* 2009;52(17):5344–55.
- Velkov T. Thermodynamics of lipophilic drug binding to intestinal fatty acid binding protein and permeation across membranes. *Mol Pharm.* 2009;6(2):557–70.
- Velkov T, Chuang S, Prankerd R, Sakellaris H, Porter CJ, Scanlon MJ. An improved method for the purification of rat liver-type fatty acid binding protein from *Escherichia coli*. *Protein Expr Purif.* 2005;44(1):23–31.
- Velkov T, Chuang S, Wielens J, Sakellaris H, Charman WN, Porter CJ, *et al.* The interaction of lipophilic drugs with intestinal fatty acid-binding protein. *J Biol Chem.* 2005;280(18):17769–76.
- Velkov T, Horne J, Laguerre A, Jones E, Scanlon MJ, Porter CJ. Examination of the role of intestinal fatty acid-binding protein in drug absorption using a parallel artificial membrane permeability assay. *Chem Biol.* 2007;14(4):453–65.
- Velkov T, Lim ML, Horne J, Simpson JS, Porter CJ, Scanlon MJ. Characterization of lipophilic drug binding to rat intestinal fatty acid binding protein. *Mol Cell Biochem.* 2009;326(1–2):87–95.
- Cummins CL, Salphati L, Reid MJ, Benet LZ. *In vivo* modulation of intestinal CYP3A metabolism by P-glycoprotein: studies using the rat single-pass intestinal perfusion model. *J Pharmacol Exp Ther.* 2003;305(1):306–14.
- Hiranpanich V, Murakoso K, Sato H. Inhibitory effect of docosahexaenoic acid (DHA) on the intestinal metabolism of midazolam: *in vitro* and *in vivo* studies in rats. *Int J Pharm.* 2008;351(1–2):133–43.
- Lane ME, Levis KA, Corrigan OI. Effect of intestinal fluid flux on ibuprofen absorption in the rat intestine. *Int J Pharm.* 2006;309(1–2):60–6.
- Poirier H, Degrace P, Niot I, Bernard A, Besnard P. Localization and regulation of the putative membrane fatty-acid transporter (FAT) in the small intestine. Comparison with fatty acid-binding proteins (FABP). *Eur J Biochem.* 1996;238(2):368–73.
- Bass NM. The cellular fatty acid binding proteins: aspects of structure, regulation, and function. *Int Rev Cytol.* 1988;111:143–84.
- Johnson BM, Chen W, Borchardt RT, Charman WN, Porter CJ. A kinetic evaluation of the absorption, efflux, and metabolism of verapamil in the autoperfused rat jejunum. *J Pharmacol Exp Ther.* 2003;305(1):151–8.
- Windmueller HG, Spaeth A. Vascular perfusion of rat small intestine for permeation and metabolism studies. In: Csazky TZ, editor. *Pharmacology of Intestinal Permeation*. Berlin: Springer-Verlag; 1984. p. 113–156.

36. Farraj NF, Davis SS, Parr GD, Stevens HNE. Absorption of progavide from aqueous solutions in a modified recirculating rat intestinal perfusion system. *Int J Pharm.* 1988;43:93–100.
37. Porter CJ, Charman SA, Charman WN. Lymphatic transport of halofantrine in the triple-cannulated anesthetized rat model: effect of lipid vehicle dispersion. *J Pharm Sci.* 1996;85(4):351–6.
38. Lacombe O, Woodley J, Solleux C, Delbos JM, Boursier-Neyret C, Houin G. Localisation of drug permeability along the rat small intestine, using markers of the paracellular, transcellular and some transporter routes. *Eur J Pharm Sci.* 2004;23(4–5):385–91.
39. Svensson US, Sandstrom R, Carlborg O, Lennernas H, Ashton M. High *in situ* rat intestinal permeability of artemisinin unaffected by multiple dosing and with no evidence of P-glycoprotein involvement. *Drug Metab Dispos.* 1999;27(2):227–32.
40. Lindahl A, Sandstrom R, Ungell AL, Lennernas H. Concentration- and region-dependent intestinal permeability of fluvastatin in the rat. *J Pharm Pharmacol.* 1998;50(7):737–44.
41. Salphati L, Childers K, Pan L, Tsutsui K, Takahashi L. Evaluation of a single-pass intestinal-perfusion method in rat for the prediction of absorption in man. *J Pharm Pharmacol.* 2001;53(7):1007–13.
42. Grassi M, Cadelli G. Theoretical considerations on the *in vivo* intestinal permeability determination by means of the single pass and recirculating techniques. *Int J Pharm.* 2001;229(1–2):95–105.
43. Trevaskis NL, Lo CM, Ma LY, Tso P, Irving HR, Porter CJ, *et al.* An acute and coincident increase in FABP expression and lymphatic lipid and drug transport occurs during intestinal infusion of lipid-based drug formulations to rats. *Pharm Res.* 2006;23(8):1786–96.
44. Bustin SA. Quantification of mRNA using real-time reverse transcription PCR (RT-PCR): trends and problems. *J Mol Endocrinol.* 2002;29(1):23–39.
45. Murakami T, Takano M. Intestinal efflux transporters and drug absorption. *Expert Opin Drug Metab Toxicol.* 2008;4(7):923–39.
46. Kunta JR, Sinko PJ. Intestinal drug transporters: *in vivo* function and clinical importance. *Curr Drug Metab.* 2004;5(1):109–24.
47. Nordskog BK, Phan CT, Nutting DF, Tso P. An examination of the factors affecting intestinal lymphatic transport of dietary lipids. *Adv Drug Deliv Rev.* 2001;50(1–2):21–44.
48. Poirier H, Niot I, Degrace P, Monnot MC, Bernard A, Besnard P. Fatty acid regulation of fatty acid-binding protein expression in the small intestine. *Am J Physiol.* 1997;273(2 Pt 1):G289–95.
49. Ockner RK, Manning JA. Fatty acid-binding protein in small intestine. Identification, isolation, and evidence for its role in cellular fatty acid transport. *J Clin Invest.* 1974;54(2):326–38.
50. Petit V, Arnould L, Martin P, Monnot MC, Pineau T, Besnard P, *et al.* Chronic high-fat diet affects intestinal fat absorption and postprandial triglyceride levels in the mouse. *J Lipid Res.* 2007;48(2):278–87.
51. Besnard P, Mallordy A, Carlier H. Transcriptional induction of the fatty acid binding protein gene in mouse liver by bezafibrate. *FEBS Lett.* 1993;327(2):219–23.
52. Hallden G, Holehouse EL, Dong X, Aponte GW. Expression of intestinal fatty acid binding protein in intestinal epithelial cell lines, hBRIE 380 cells. *Am J Physiol.* 1994;267(4 Pt 1):G730–43.
53. Schoonjans K, Martin G, Staels B, Auwerx J. Peroxisome proliferator-activated receptors, orphans with ligands and functions. *Curr Opin Lipidol.* 1997;8(3):159–66.
54. Tuleu C, Newton M, Rose J, Euler D, Saklatvala R, Clarke A, *et al.* Comparative bioavailability study in dogs of a self-emulsifying formulation of progesterone presented in a pellet and liquid form compared with an aqueous suspension of progesterone. *J Pharm Sci.* 2004;93(6):1495–502.
55. Thummel KE, O'Shea D, Paine MF, Shen DD, Kunze KL, Perkins JD, *et al.* Oral first-pass elimination of midazolam involves both gastrointestinal and hepatic CYP3A-mediated metabolism. *Clin Pharmacol Ther.* 1996;59(5):491–502.
56. Ghosal A, Satoh H, Thomas PE, Bush E, Moore D. Inhibition and kinetics of cytochrome P4503A activity in microsomes from rat, human, and cDNA-expressed human cytochrome P450. *Drug Metab Dispos.* 1996;24(9):940–7.
57. van Waterschoot RA, van Herwaarden AE, Lagas JS, Sparidans RW, Wagenaar E, van der Kruijssen CM, *et al.* Midazolam metabolism in cytochrome P450 3A knockout mice can be attributed to up-regulated CYP2C enzymes. *Mol Pharmacol.* 2008;73(3):1029–36.
58. Chen M, Yang Y, Braunstein E, Georgeson KE, Harmon CM. Gut expression and regulation of FAT/CD36: possible role in fatty acid transport in rat enterocytes. *Am J Physiol Endocrinol Metab.* 2001;281(5):E916–23.
59. de Vogel-van den Bosch HM, de Wit NJ, Hooiveld GJ, Vermeulen H, van der Veen JN, Houten SM, *et al.* A cholesterol-free, high-fat diet suppresses gene expression of cholesterol transporters in murine small intestine. *Am J Physiol Gastrointest Liver Physiol.* 2008;294(5):G1171–80.
60. Cao J, Hawkins E, Brozinick J, Liu X, Zhang H, Burn P, *et al.* A predominant role of acyl-CoA:monoacylglycerol acyltransferase-2 in dietary fat absorption implicated by tissue distribution, subcellular localization, and up-regulation by high fat diet. *J Biol Chem.* 2004;279(18):18878–86.
61. Hernandez Vallejo SJ, Alqub M, Luquet S, Cruciani-Guglielmacci C, Delerive P, Lobaccaro JM, *et al.* Short-term adaptation of postprandial lipoprotein secretion and intestinal gene expression to a high-fat diet. *Am J Physiol Gastrointest Liver Physiol.* 2009;296(4):G782–92.
62. Fisher EA, Anbari A, Klurfeld DM, Kritchevsky D. Independent effects of diet and nutritional status on apoprotein B gene expression in rabbit. *Arteriosclerosis.* 1988;8(6):797–803.
63. Goda T, Yasutake H, Takase S. Dietary fat regulates cellular retinol-binding protein II gene expression in rat jejunum. *Biochim Biophys Acta.* 1994;1200(1):34–40.
64. Schmitz G, Langmann T. Metabolic learning in the intestine: adaptation to nutrition and luminal factors. *Horm Metab Res.* 2006;38(7):452–4.
65. Winiwarter S, Bonham NM, Ax F, Hallberg A, Lennernas H, Karlen A. Correlation of human jejunal permeability (*in vivo*) of drugs with experimentally and theoretically derived parameters. A multivariate data analysis approach. *J Med Chem.* 1998;41(25):4939–49.
66. Hirunpanich V, Murakoso K, Sato H. Inhibitory effect of docosahexaenoic acid (DHA) on the intestinal metabolism of midazolam: *in vitro* and *in vivo* studies in rats. *Int J Pharm.* 2008;351(1–2):133–43.